Interacting boson-fermion model analysis of beta decay in $A = 195$ and 197 nuclei

P. Navrátil and J. Dobeš
Institute of Nuclear Physics, Czechoslovak Academy of Sciences, 250 68 Řež, Czechoslovakia
(Received 8 September 1987)

The interacting boson-fermion model is used to analyze beta decay. The beta transition operator in the boson-fermion space is constructed with the parameters obtained from microscopic considerations. The ft values are calculated for the first nonunique forbidden transitions between states based on natural parity orbitals in the decays of $^{195}\mathrm{Ir}\rightarrow{}^{195}\mathrm{Pt}$, $^{195}\mathrm{Au}\rightarrow{}^{195}\mathrm{Pt}$, $^{195}\mathrm{Hg}\rightarrow{}^{195}\mathrm{Au}$, $^{197}\mathrm{Pt}\rightarrow{}^{197}\mathrm{Au}$, and $^{197}\mathrm{Hg}\rightarrow{}^{197}\mathrm{Au}$. The structure of the odd-neutron nuclei is described in the U(6)⊗U(12) boson-fermion symmetry limit. For the odd-proton nuclei, three different approaches, in particular the U(6)⊗U(4) symmetry, the U(6)⊗U(20) symmetry, and the perturbed U(6)⊗U(4) scheme, are compared. The calculated ft values are very sensitive to details of nuclear wave functions, the best results being obtained with the perturbed U(6)⊗U(4) scheme. Phase ambiguities in nuclear wave functions can be disentangled from beta decay analysis. The exchange terms in the boson-fermion transition operator, which take into account the Pauli principle between the odd-nucleon and nucleons forming the even-even collective core, proved to be quite important.

I. INTRODUCTION

Remarkable success has been achieved in the description of collective nuclear states in medium and heavy mass nuclei within the interacting boson model[1] (IBM) and the interacting boson-fermion model[2] (IBFM). The IBM and IBFM have been confronted with experiment by comparing energy levels, electromagnetic properties, and one- and two-nucleon transfer spectroscopic strengths. Double beta decay with the IBM wave functions was also studied.[3] No IBM and/or IBFM investigation has till now been made for single beta decay observables. From these especially, the ft value, depending on the absolute magnitudes of form factors, is very sensitive to details of nuclear structure calculations.

This particular situation in the IBM/IBFM reflects the situation in collective nuclear models generally. Beta decay is not often analyzed in these models, presumably for two reasons. (i) The beta decay study in even systems needs a knowledge of the structure of odd-odd nuclei, which are seldom investigated in collective models and the understanding of which is not too satisfactory. As concerning odd systems, pairs of proton-neutron odd-even and even-odd nuclei have not been frequently considered together in one study. Particularly, in the IBFM only a few such pairs have been investigated at all.

(ii) The agreement between theory and experiment is usually worse for nuclear beta decay observables than for other nuclear characteristics. The ft value often depends on an interplay of several matrix elements. Relatively small variations in the matrix elements can change the resulting ft value considerably.

We refer to the book by Behrens and Bühring[4] for discussion of and references to beta decay studies in collective nuclei. The agreement between theoretical and experimental ft values is not very good in these regions. Differences between calculated and measured $\log ft$ values of about 1 are sometimes considered even as satisfactory. Here, we mention the work of Bogdan and collaborators on some transitional odd mass nuclei (including the $A = 195$ system, which we also investigate in the following).[5] In Ref. 5, the differences between theory, using the nonaxial rotor model combined with the decoupling model, and experiment lay in the limits

$$-1.32 \leq \log ft_{\mathrm{expt}} - \log ft_{\mathrm{theor.}} \leq 2.5 \ .$$

On the other hand, for nuclei where shell model calculations are available, quite a good qualitative accounting of observed ft values is obtained. Not only allowed transitions in light nuclei, but also forbidden transitions in the lead region have been dealt with reasonably well. It is, therefore, appealing and interesting to prospect beta decay in collective nuclei more intensively.

In the present paper we calculate the ft values for the $A = 195$ and $A = 197$ systems. The decays of $^{195}\mathrm{Ir}\rightarrow{}^{195}\mathrm{Pt}$, $^{195}\mathrm{Au}\rightarrow{}^{195}\mathrm{Pt}$, $^{195}\mathrm{Hg}\rightarrow{}^{195}\mathrm{Au}$, $^{197}\mathrm{Pt}\rightarrow{}^{197}\mathrm{Au}$, and $^{197}\mathrm{Hg}\rightarrow{}^{197}\mathrm{Au}$ are studied. Only the first nonunique forbidden transitions between states based on natural parity orbitals are considered (contrary to Ref. 5 where the $^{195}\mathrm{Ir}\rightarrow{}^{195}\mathrm{Pt}$ decay between intruder orbitals was investigated).

The nuclear structure in the mass region studied is rather complicated and numerous degrees of freedom have been invoked to understand it. In terms of the IBM, this region is a good example of realization of the O(6) boson symmetry.[6] The boson symmetry concept has been extended to odd nuclei, by recognizing boson-fermion (BF) dynamical symmetries in the IBFM. The BF symmetry based on the group $\mathrm{U}^B(6)\otimes\mathrm{U}^F(4)$ has been suggested for the odd-proton nuclei with $A = 195$ and 197,[7] whereas the $\mathrm{U}^B(6)\otimes\mathrm{U}^F(12)$ symmetry has been found to be relevant for odd-neutron nuclei.[8] We start our calculations of beta decay with these BF symmetry limit descriptions of nuclear states. Then, we try to refine upon results by using either the extended $\mathrm{U}^B(6)\otimes\mathrm{U}^F(20)$ symmetry[9] or the perturbed $\mathrm{U}^B(6)\otimes\mathrm{U}^F(4)$ scheme.[10]

II. BETA DECAY FORMALISM

At present, a rather reliable formalism for treating nuclear beta decay exists. It is based on the so-called elementary particle treatment formulated in terms of form factors. Sufficiently precise methods have also been developed for handling the Coulomb interaction. The formalism is explained and discussed extensively in the book by Behrens and Bühring[4] which we rely on and the notation of which is closely followed further.

We study the first nonunique forbidden beta transitions with the spin selection rule

$$\Delta J=0,1$$

and the parity selection rule

$$\pi_i\pi_f=-1 \ .$$

For them we have (the natural units $\hbar=c=m_e=1$ are used throughout the present section)

$$ft=\frac{2\pi^3\ln 2}{G_\beta^2(A_0^2+C_0^2)} \ . \tag{1}$$

The beta decay coupling constant is denoted as G_β. The quantities A_0 and C_0 are related to the total angular momentum transfer 0 and 1 and we redenote them in the following as M_0 and M_1, respectively. They can be expressed through the form factors F with the dominant terms only included as

$$M_0={}^AF^{(0)}_{000}\mp\tfrac{1}{3}\alpha Z\,{}^AF^{(0)}_{011}(1,1,1,1)-\tfrac{1}{3}W_0R\,{}^AF^{(0)}_{011} \ , \tag{2a}$$

$$\begin{aligned}M_1=&-{}^VF^{(0)}_{101}\mp\tfrac{1}{3}\alpha Z\sqrt{1/3}\,{}^VF^{(0)}_{110}(1,1,1,1)\\&-\tfrac{1}{3}W_0R\sqrt{1/3}\,{}^VF^{(0)}_{110}\\&\mp\tfrac{1}{3}\alpha Z\sqrt{2/3}\,{}^AF^{(0)}_{111}(1,1,1,1)+\tfrac{1}{3}W_0R\sqrt{2/3}\,{}^AF^{(0)}_{111} \ .\end{aligned} \tag{2b}$$

Here and in Eqs. (3) below, the upper (lower) sign applies to β^- (β^+ and electron capture) decay, W_0 is the maximum energy of the beta particles (in the case of electron capture, the maximum total positron decay energy plus the electron mass minus the binding energy of the bound electron in the parent atom), Z is the atomic number of the daughter nucleus (in the case of electron capture of the parent nucleus), R is the nuclear charge radius, and α denotes the fine structure constant. In the form factor notation ${}^{A,V}F^{(0)}_{KLs}$, A or V relate to the axial or vector character, K, L, and s are the transferred total angular momentum, angular momentum, and spin, respectively.

Neglecting the induced terms and using the impulse approximation which is a usual and justified procedure for the considered transitions, we write the form factors in terms of nuclear matrix elements as

$${}^VF^{(0)}_{KLs}=(-)^{K-L}\,{}^V\mathcal{M}^{(0)}_{KLs} \ , \tag{3a}$$

$${}^AF^{(0)}_{KLs}=\pm(-)^{K-L}\lambda\ {}^A\mathcal{M}^{(0)}_{KLs} \ , \tag{3b}$$

where λ is the negative ratio of the axial vector to vector coupling constants. The nuclear matrix elements are expressed in terms of the reduced matrix elements of the one-body operator

$$\begin{aligned}{}^{V,A}\mathcal{M}^{(0)}_{KLs}=&-\hat{K}^{-1}\sum_{j_fj_i}\langle j_f\|{}^{V,A}O_{KLs}\|j_i\rangle\\&\times\langle J_f\|(c^\dagger_{j_f}\tilde{c}_{j_i})^{(K)}\|J_i\rangle \ .\end{aligned} \tag{4}$$

Here, $\hat{K}=\sqrt{2K+1}$, $J_i(J_f)$ denote the initial (final) nuclear state, $c^\dagger_j$ is the shell model single-particle creation operator, $\tilde{c}_{jm}=(-)^{j-m}c_{j-m}$, the angular momentum coupling is denoted by $(\ )^{(K)}$, and the sum runs over the initial neutron (proton) single-particle states j_i and the final proton (neutron) single-particle states j_f in the case of β^- (β^+ and electron capture) decay. The single-particle reduced matrix elements $\langle\|O_{KLs}\|\rangle$ are tabulated in Ref. 4 and depend on a geometrical factor and the radial integrals Ω_1, Ω_2, and Ω_3, given in the nonrelativistic limit as

$$\Omega_1=\int_0^\infty g_f(E_i-E_f-V_i+V_f)rg_ir^2dr \ , \tag{5a}$$

$$\Omega_2=\int_0^\infty g_f\frac{r}{R}g_ir^2dr \ , \tag{5b}$$

$$\Omega_3=\int_0^\infty g_f\frac{r}{R}I(1,1,1,1;r)g_ir^2dr \ . \tag{5c}$$

Here g is the solution of the Schrödinger single-particle radial equation, E and V are the energy and potential related to the single-particle state. For the function I in the model of a uniform charge distribution we have

$$I(1,1,1,1;r)=\begin{cases}\dfrac{3}{2}-\dfrac{3}{10}\left[\dfrac{r}{R}\right]^2 & \text{if } 0\le r\le R\\[2ex] \dfrac{3}{2}\dfrac{R}{r}-\dfrac{3}{10}\left[\dfrac{R}{r}\right]^3 & \text{if } R\le r \ .\end{cases} \tag{6}$$

Summarizing the above equations we see that the quantities M_0 and M_1 may be expressed as the reduced matrix elements

$$M_K=\langle J_f\|T^{(K)}\|J_i\rangle \tag{7}$$

of the beta transition operator

$$T^{(K)}=\sum_{j_fj_i}\xi^{(K)}_{j_fj_i}(c^\dagger_{j_f}\tilde{c}_{j_i})^{(K)} \ . \tag{8}$$

The quantities ξ are given as combinations of the reduced matrix elements $\langle\|O_{KLs}\|\rangle$ with coefficients determined by Eqs. (2)–(4).

A question arises about the renormalization of weak form factors in finite nuclei. Two mechanisms are important in that context: the meson exchange effects and the core polarization effects. The former mechanism was shown to increase the axial-charge form factor ${}^AF^{(0)}_{000}$.[11] This implies in some cases, and especially for the $0^+\leftrightarrow 0^-$ transitions, a large decrease of the resulting ft value. The inclusion of the core polarization effects rises usually the calculated ft values.[12–15]

On the other hand, the ft values for the beta transitions in systems close to the magic ^{208}Pb nucleus can be explained satisfactorily using the free-nucleon coupling

constants.[4] This does not mean that the exchange and core polarization effects are small but perhaps this indicates certain cancellation of both effects. In this respect, the free-nucleon coupling constants might be considered as close to the effective ones. In the present study, we follow Ref. 4 adopting the procedure with the free-nucleon values

$$G_\beta = 2.996 \times 10^{-12}$$

and

$$\lambda = 1.25 \ .$$

It should be kept in mind, however, that in more detailed studies, and for a perfect explanation of experimental data, both the exchange and core polarization effects should be taken into account explicitly.

The radial integrals (5) are calculated with the single-particle wave functions obtained from the Woods-Saxon potential. The global parameters of Bear and Hodgson[16] giving a good overall fit to the centroid binding energies of many single-particle states in nuclei from ^{40}Ca to ^{208}Pb are used. The integrals are shown in Table I. We have found that for the transitions considered they are less sensitive to different single-particle potentials than the integrals for the $2g_{9/2} \rightarrow 1h_{9/2}$ transition discussed in Ref. 4.

III. BETA TRANSITION OPERATOR IN BOSON-FERMION SPACE

In the IBFM one treats odd-A nuclei by coupling single-quasiparticle degrees of freedom to a system of s and d bosons describing the even-even core. An image of the beta transition operator (8) in the boson-fermion (BF) space has to be constructed in order to calculate beta transition matrix elements in the IBFM. To do that we will make use of the pseudoparticle creation operator $c_j^\dagger$ as was introduced in Refs. 17 and 18:

$$c_j^\dagger = u_j a_j^\dagger + v_j \frac{1}{\sqrt{N}} s^\dagger \tilde{a}_j + \sum_{j'} u_j \bar{\beta}_{j'j} \sqrt{10}/\hat{j} (d^\dagger \tilde{a}_{j'})^{(j)} - \sum_{j'} v_j 1/\sqrt{N}\, \bar{\beta}_{j'j} \sqrt{10}/\hat{j} s^\dagger (\tilde{d} a_{j'}^\dagger)^{(j)} \ . \quad (9)$$

Equation (9) represents the lowest order terms of the image of the shell model single-particle creation operator $c_j^\dagger$ in the BF space. The single-quasiparticle creation operator is denoted as $a_j^\dagger$, $s^\dagger$ and $d^\dagger$ are the s- and d-boson creation operators, and N is the number of bosons considered in the even-even core. The coefficients u_j, v_j, and $\bar{\beta}_{j'j}$ are parameters in a pure phenomenological approach. They can be, however, specified by using a microscopic interpretation of the IBM in which the s and d bosons are images of the collective fermion S and D pairs. The coefficients u_j, v_j, and $\bar{\beta}_{j'j}$ are then related to the internal structure of the S and D pairs. More specifically, the coefficients u_j and $v_j = (1-u_j^2)^{1/2}$ are usually taken as the occupation amplitudes of spherical shell model orbits and play the same role as the corresponding quantities in the Bardeen-Cooper-Schrieffer (BCS) theory.[19]

Since neutron and proton operators commute, the image of the beta transition operator in the BF space is simply constructed by replacing the shell model operators $c_{j_f}^\dagger$ and $\tilde{c}_{j_i}$ in Eq. (8) by the pseudoparticle operators (9). Only the terms that are up to the first order in the d-boson operators are retained in Eqs. (10) and (11) below. To treat consistently terms with two d-boson operators, one should take into account also terms that are quadratic in the d bosons in the BF image of the single-particle operator. At present, no evaluation of the these higher order terms exists. Moreover, it is plausible to assume that the influence of terms in the BF transition operator

TABLE I. Radial integrals Ω_1, Ω_2, and Ω_3 [Eq. (5)] for beta decay single-particle matrix elements. The upper (lower) sign applies to β^- (β^+) decay. The natural units $\hbar = c = m_e = 1$ are used.

	ν \ π	$3s_{1/2}$	$2d_{3/2}$	$2d_{5/2}$	$1g_{7/2}$
Ω_1	$3p_{1/2}$	± 0.173	∓ 0.146		
	$3p_{3/2}$	± 0.178	∓ 0.152	∓ 0.144	
	$2f_{5/2}$		± 0.194	± 0.186	∓ 0.113
	$2f_{7/2}$			± 0.197	∓ 0.128
	$1h_{9/2}$				± 0.214
Ω_2	$3p_{1/2}$	0.590	-0.397		
	$3p_{3/2}$	0.579	-0.379	-0.399	
	$2f_{5/2}$		0.693	0.701	-0.253
	$2f_{7/2}$			0.684	-0.193
	$1h_{9/2}$				0.783
Ω_3	$3p_{1/2}$	0.730	-0.461		
	$3p_{3/2}$	0.716	-0.438	-0.467	
	$2f_{5/2}$		0.879	0.891	-0.278
	$2f_{7/2}$			0.872	-0.200
	$1h_{9/2}$				1.010

diminishes with the increasing number of the d-boson operators included.[18,20]

We specify the transition operator for β^- decay, i.e., indices $i \equiv \nu$ and $f \equiv \pi$ relate to neutron and proton operators, respectively. Keeping only the terms which are relevant to beta decay in odd-mass nuclei and connecting the corresponding quasiparticle spaces, we obtain two kinds of the beta transition operators in the BF space. The first kind conserves the numbers of the proton and neutron bosons separately,

$$T_{\mathrm{I}}^{(K)} = -\sum_{j_\pi j_\nu} \xi_{j_\pi j_\nu}^{(K)} \left\{ u_{j_\pi} u_{j_\nu} (a_{j_\pi}^\dagger \tilde{a}_{j_\nu})^{(K)} - \sum_{j'_\nu} u_{j_\pi} v_{j_\nu} \bar{\beta}_{j'_\nu j_\nu} \sqrt{10/N_\nu} \frac{1}{\hat{j}_\nu} s_\nu [a_{j_\pi}^\dagger (d_\nu^\dagger \tilde{a}_{j'_\nu})^{(j_\nu)}]^{(K)} \right.$$
$$\left. - \sum_{j'_\pi} v_{j_\pi} u_{j_\nu} \bar{\beta}_{j'_\pi j_\pi} \sqrt{10/N_\pi} \frac{1}{\hat{j}_\pi} s_\pi^\dagger [(\tilde{d}_\pi a_{j'_\pi}^\dagger)^{(j_\pi)} \tilde{a}_{j_\nu}]^{(K)} \right\} , \tag{10}$$

and describes beta transitions between nuclei with the same even-even core

$$N_\pi, N_\nu, n_\nu = 1 \rightarrow N_\pi, N_\nu, n_\pi = 1 ,$$

$n_\pi (n_\nu)$ being the single-particle number. The second kind changes one neutron boson into one proton boson together with the conversion of the odd fermion,

$$T_{\mathrm{II}}^{(K)} = \sum_{j_\pi j_\nu} \xi_{j_\pi j_\nu}^{(K)} \left\{ v_{j_\pi} v_{j_\nu} \sqrt{1/N_\pi N_\nu} s_\pi^\dagger s_\nu (\tilde{a}_{j_\pi} a_{j_\nu}^\dagger)^{(K)} + \sum_{j'_\pi} u_{j_\pi} v_{j_\nu} \bar{\beta}_{j'_\pi j_\pi} \sqrt{10/N_\nu} \frac{1}{\hat{j}_\pi} s_\nu [(d_\pi^\dagger \tilde{a}_{j'_\pi})^{(j_\pi)} a_{j_\nu}^\dagger]^{(K)} \right.$$
$$\left. + \sum_{j'_\nu} v_{j_\pi} u_{j_\nu} \bar{\beta}_{j'_\nu j_\nu} \sqrt{10/N_\pi} \frac{1}{\hat{j}_\nu} s_\pi^\dagger [\tilde{a}_{j_\pi} (\tilde{d}_\nu a_{j'_\nu}^\dagger)^{(j_\nu)}]^{(K)} \right\} , \tag{11}$$

and is relevant to processes in which parent and daughter nuclei have the different even-even cores

$$N_\pi - 1, N_\nu, n_\pi = 1 \rightarrow N_\pi, N_\nu - 1, n_\nu = 1 .$$

Other kinds of the beta transition operator containing combinations $a_\pi^\dagger a_\nu^\dagger$ or $\tilde{a}_\pi \tilde{a}_\nu$ describe beta decay in even mass systems which are not studied here.

Individual terms in the transition operators (10) and (11) are graphically represented in Figs. 1 and 2. The first direct term of Eq. (10) is the usual quasiparticle beta transition operator with the pairing suppression factor $u_\pi u_\nu$.[21] The other terms in Eq. (10) are the exchange terms which take into account the Pauli principle between the odd nucleon and nucleons constituting the even-even collective core. The state of the even-even core is changed by the action of these terms. The microscopic interpretation of the IBM enables us to evaluate the exchange terms explicitly.

In the second kind of the transition operator (11), an action on the collective even-even core is introduced in all three terms shown in Fig. 2. When we pass from the particle-like description to the hole-like description of valence nucleons, the second kind (11) transfers into the

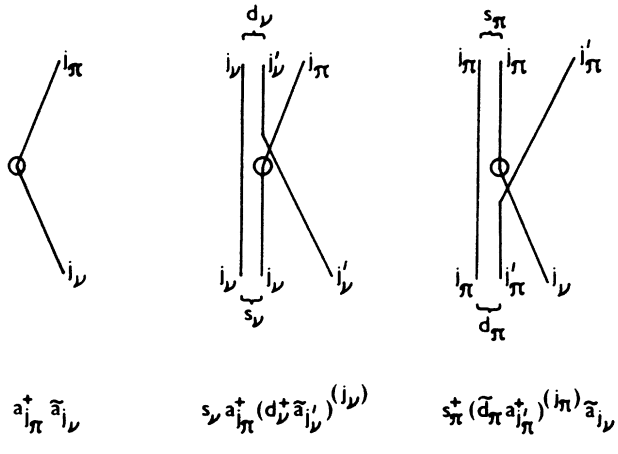

FIG. 1. Diagrams for the first-type IBFM beta transition operator [Eq. (10)]. The elementary beta process is marked by a circle.

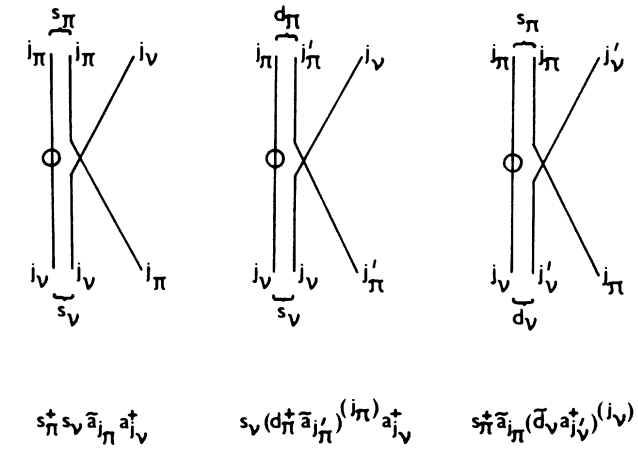

FIG. 2. The same as Fig. 1, but for the second-type IBFM beta transition operator [Eq. (11)].

first kind (10), and vice versa. The direct term has then the pairing suppression factor $v_\pi v_\nu$.[21]

In connection with the particlelike and holelike descriptions of valence nucleons, we should mention one point which seems to be sometimes missed. When we use the holelike picture, the occupancies u_j and v_j in Eq. (9) relate to holes, i.e., $u_j^2=1$ in the case of no hole or equivalently of a valence shell filled with particles. In calculations of the occupancies from the BCS theory we have either to use the number of the holes or to interchange u_j and v_j after calculating with the true particle number.

The operators (10) and (11) are written in the IBFM-2 formalism with the proton and neutron bosons distinguished. In calculations, however, we shall use the IBFM-1 version with one kind of boson. We have, therefore, to project Eqs. (10) and (11) onto the IBFM-1 space. Applying the usual projection method,[17] in which matrix elements between corresponding IBFM-2 and IBFM-1 states are equated, we get the IBFM-1 form of the transition operators by replacing in Eq. (10)

$$s_\nu d_\nu^\dagger \rightarrow (N_\nu/N) s d^\dagger , \tag{12a}$$

$$s_\pi^\dagger \tilde{d}_\pi \rightarrow (N_\pi/N) s^\dagger \tilde{d} , \tag{12b}$$

and in Eq. (11)

$$s_\pi^\dagger s_\nu \rightarrow \sqrt{N_\pi N_\nu}/(N-1) s^\dagger s \approx \sqrt{N_\pi N_\nu} , \tag{12c}$$

$$s_\nu d_\pi^\dagger \rightarrow \sqrt{N_\pi N_\nu}/(N-1) s d^\dagger , \tag{12d}$$

$$s_\pi^\dagger \tilde{d}_\nu \rightarrow \sqrt{N_\pi N_\nu}/(N-1) s^\dagger \tilde{d} , \tag{12e}$$

with $N=N_\pi+N_\nu$. The operator $s^\dagger s$ in Eq. (12c) is replaced by the expression $(N-1-d^\dagger\cdot d)$, in which we neglect the term containing two d-boson operators for the reasons discussed above. We get then completely symmetric forms of the first and second kinds of the transition operators with respect to the particlelike and holelike descriptions.

In the nuclei with $A=195$ and 197 both protons and neutrons have holelike character. The occupation amplitudes u_j and v_j used in the transition operators (10) and (11) are calculated from the BCS theory with the gap $\Delta=135/A$. The single-particle energies for neutrons are taken from Ref. 20 and for protons they are obtained from the global single-nucleon potential.[16] The occupation probabilities v_j^2 (for holes) are given in Tables II and III.

The coefficients $\bar{\beta}_{jj'}$, related to the structure of the D-collective pair, are obtained under the assumption that the D state exhausts the full valence $E2$ strength with the effect of nondegeneracy of single-nucleon orbits taken into account[22]

$$\bar{\beta}_{jj'}=\mathcal{N}\frac{1}{\varepsilon_j+\varepsilon_{j'}-E_D}(u_j v_{j'}+v_j u_{j'})\langle j\|Y^{(2)}\|j'\rangle \tag{13}$$

with the normalization

$$\sum_{jj'}(\bar{\beta}_{jj'})^2=1 .$$

The quasiparticle energies ε_j from the BCS calculations are given in Tables II and III. The energies E_D of the D states relative to the S states are estimated from the 2^+ state energies of the double-magic plus two hole nuclei ^{206}Pb and ^{206}Hg to be $E_D=0.80$ MeV and $E_D=1.07$ MeV for neutron and proton pairs, respectively.

All valence shells for protons ($Z=50-82$) and neutrons ($N=82-126$) are considered in the calculation of the normalization of the coefficients $\bar{\beta}_{jj'}$ and in the transition operators (10) and (11).

IV. NUCLEAR STATES

A. Odd-neutron nuclei — U(6)⊗U(12) symmetry

Low-lying negative parity states in the odd-neutron Pt and Hg isotopes can be described by coupling a neutron hole in the $p_{1/2}$, $p_{3/2}$, and $f_{5/2}$ orbits to an even-even core. This suggests the use of the BF symmetries based on the group $U^B(6)\otimes U^F(12)$.[8] Since the even-even Pt core is a good example of the O(6) boson symmetry, the symmetry limit

TABLE II. Single-particle energies E_j, quasiparticle energies ε_j, and occupation probabilities v_j^2 for neutron holes.

		$3p_{1/2}$	$2f_{5/2}$	$3p_{3/2}$	$2f_{7/2}$	$1h_{9/2}$	$1i_{13/2}$
	E_j (MeV)	0.00	0.59	0.94	2.44	3.51	1.54
^{195}Hg	ε_j (MeV)	1.09	0.74	0.70	1.75	2.76	0.99
	v_j^2	0.89	0.67	0.43	0.04	0.02	0.14
^{195}Pt	ε_j (MeV)	0.95	0.69	0.73	1.88	2.93	1.10
^{197}Hg	v_j^2	0.84	0.54	0.33	0.04	0.01	0.11
^{197}Pt	ε_j (MeV)	0.81	0.70	0.86	2.13	3.16	1.31
	v_j^2	0.76	0.38	0.20	0.03	0.01	0.07

TABLE III. Single-particle energies E_j, quasiparticle energies ε_j, and occupation probabilities v_j^2 for proton holes.

		$3s_{1/2}$	$2d_{3/2}$	$2d_{5/2}$	$1g_{7/2}$	$1h_{11/2}$
	E_j (MeV)	0.00	0.70	2.50	4.11	2.11
^{195}Ir	ε_j (MeV)	0.89	0.71	2.06	3.62	1.70
	v_j^2	0.81	0.40	0.03	0.01	0.04
^{195,197}Au	ε_j (MeV)	0.69	0.99	2.61	4.18	2.24
	v_j^2	0.49	0.14	0.02	0.01	0.02

$$\mathrm{U}^B(6)\otimes\mathrm{U}^F(12)\supset\mathrm{U}^B(6)\otimes\mathrm{U}^F(6)\otimes\mathrm{SU}^F(2)\supset\mathrm{U}^{\mathrm{BF}}(6)\otimes\mathrm{SU}^F(2)$$
$$\supset\mathrm{SO}^{\mathrm{BF}}(6)\otimes\mathrm{SU}^F(2)\supset\mathrm{SO}^{\mathrm{BF}}(5)\otimes\mathrm{SU}^F(2)\supset\mathrm{SO}^{\mathrm{BF}}(3)\otimes\mathrm{SU}^F(2)\supset\mathrm{spin}(3) \tag{14}$$

has been discussed[23,24] and found actually to reproduce the structure of the ^{195,197}Pt isotopes very well.[25]

For the even-even Hg isotopes both the O(6) limit and the U(5) limit have been discussed.[26] In addition to the limit (14), also the BF symmetries with the U(5) subgroup

$$\mathrm{U}^B(6)\otimes\mathrm{U}^F(12)\supset\mathrm{U}^B(6)\otimes\mathrm{U}^F(6)\otimes\mathrm{SU}^F(2)\supset\begin{array}{c}\nearrow\ \mathrm{U}^{\mathrm{BF}}(6)\otimes\mathrm{SU}^F(2)\ \searrow\\ \searrow\ \mathrm{U}^B(5)\otimes\mathrm{U}^F(5)\otimes\mathrm{SU}^F(2)\ \nearrow\end{array}\supset\mathrm{U}^{\mathrm{BF}}(5)\otimes\mathrm{SU}^F(2)$$

$$\supset\mathrm{SO}^{\mathrm{BF}}(5)\otimes\mathrm{SU}^F(2)\supset\mathrm{SO}^{\mathrm{BF}}(3)\otimes\mathrm{SU}^F(2)\supset\mathrm{spin}(3) \tag{15}$$

has been applied to ^{195,197}Hg.[23,27] The analysis of single-nucleon-transfer strengths prefers the U(5) limit (15) slightly.[27]

The wave functions of the O(6) limit (14) are tabulated in Ref. 23 in which the pairing operator in the form $P^\dagger=s^\dagger s^\dagger+d^\dagger d^\dagger$ is used.[28] Throughout the present paper we use the more usual choice[20,24] $P^\dagger=s^\dagger s^\dagger-d^\dagger d^\dagger$, which is also more natural from the viewpoint of the microscopically suggested proton-neutron IBM-2 version. The signs of some components of wave functions in Table XV of Ref. 23 are modified accordingly.

The wave functions of the U(5) limit (15) are also given in Ref. 23. For the Hg ground states, only which we need in beta decay calculations, there is no difference between two alternative chains shown in Eq. (15).

The phase ambiguity in the O(6) BF symmetry limit (14) was noticed in Ref. 20. It concerns the relative sign $\phi=\pm1$ with which the bosonic and fermionic terms are added to obtain the quadrupole generators. In the wave functions, this phase transformation means a change of the relative signs between components with even and odd numbers of the d bosons. Energy levels are invariant and electromagnetic transition probabilities do not change much under the phase ϕ. The proper sign could be determined from the sign of quadrupole moments, which are, however, unknown experimentally in the odd Pt and Hg isotopes.

On the other hand, we can estimate the phase ϕ from the microscopic approach to the IBFM Hamiltonian with the BF symmetry (14).[20] It was shown that in addition to the usual boson-fermion interaction derived from the quadrupole-quadrupole proton-neutron interaction, also the boson-fermion image of the quadrupole pairing interaction between like nucleons has to be taken into account. The coefficient η of the $\mathrm{SO}^{\mathrm{BF}}$ (6) quadratic Casimir operator, appearing in the BF symmetry Hamiltonian, is related to the strengths of the quadrupole-quadrupole force Γ_0 and the quadrupole pairing force V_2 by (the notation of Ref. 20 is followed)

$$\eta=-\phi\tfrac{1}{8}\sqrt{5/\pi}[\Gamma_0(u_0u_2-v_0v_2)+\Lambda_0''v_0u_2+\Lambda_0'u_0v_2]\ . \tag{16}$$

Here, the quantities Λ_0' and Λ_0'' are proportional to the strength V_2 and are of opposite signs, $v_0^2=v_{1/2}^2$ and $v_2^2=\frac{1}{2}(v_{3/2}^2+v_{5/2}^2)$. It follows from the analysis of Ref. 20 that in order for the BF symmetry to be realized, the relation $\Lambda_0'\approx-\Lambda_0''\approx\frac{1}{2}\Gamma_0$ has to hold approximately. The parameter η is negative from the BF symmetry analysis of nuclear spectra.[20,25] Taking in Eq. (16) the positive strength Γ_0 (Ref. 20) and the occupation probabilities from Table II, we find immediately that $\phi=-1$ is suggested from the microscopic approach. We use this phase in the calculations of Sec. V, unless stated otherwise.

B. Odd-proton nuclei—U(6)⊗U(4) symmetry

For the description of positive parity states in the Ir and Au isotopes, the dynamical BF symmetry based on the $U^B(6)\otimes U^F(4)$ group has been suggested. This symmetry arises when a $d_{3/2}$ proton hole is coupled to a boson core which has the O(6) symmetry. The corresponding group decomposition is[7]

$$U^B(6)\otimes U^F(4)\supset SO^B(6)\otimes SU^F(4)\supset \text{spin}(6)\supset \text{spin}(5)\supset \text{spin}(3)\ . \tag{17}$$

The Hamiltonian of the symmetry limit (17) is written in terms of the quadratic Casimir operators of groups spin(6), spin (5), and spin (3) as[7,29]

$$H=-AC_6+BC_5+CC_3\ . \tag{18}$$

The wave functions for the U(6)⊗U(4) limit have been obtained from isoscalar factors of Ref. 7.

An experimental evidence for the BF symmetry (17) has been discussed for ^{195}Ir,[10,30] ^{195}Au,[31] and ^{197}Au.[32] The symmetry limit can explain well a large part of experimental data. The concept of the single $d_{3/2}$ shell appears, however, to be of limited applicability, especially when single-particle transfer strengths are considered.[10,33] An influence of other valence shells, and particularly of the $s_{1/2}$ level, is expected to be important.

Similarly, to the U(6)⊗U(12) case, a phase ambiguity in the symmetry limit (17) occurs.[29] It is again connected with the relative sign $\Psi=\pm 1$ of the bosonic and fermionic terms in the quadrupole generator and cannot be disentangled from energy levels and electromagnetic transition probabilities.

In the microscopic approach of Ref. 29, the coefficient A in the Hamiltonian (18) is related to the quadrupole-quadrupole strength Γ_0 by

$$A=-\Psi 2\Gamma_0(u^2_{3/2}-v^2_{3/2})\langle \tfrac{3}{2}\|Y^{(2)}\|\tfrac{3}{2}\rangle\ . \tag{19}$$

It follows from analysis of energy levels that A is positive. Using then the occupation probabilities from Table III we obtain the microscopic estimate for the phase $\Psi=+1$. We use this phase in calculations of Sec. V, unless stated otherwise.

C. Odd-proton nuclei—U(6)⊗U(20) symmetry

The BF symmetry scheme based on the group $U^B(6)\otimes U^F(20)$ has been suggested and applied to the Au isotopes in order to include valence shells other than only the $d_{3/2}$ level.[9,33] In this approach, all positive parity levels in the $Z=50$–82 shell, i.e., $s_{1/2}$, $d_{3/2}$, $d_{5/2}$, and $g_{7/2}$, are coupled to the O(6) boson core. The group chain considered is

$$U^B(6)\otimes U^F(20)\supset SO^B(6)\otimes SU^F(4)\supset \text{spin}(6)\supset \text{spin}(5)\supset \text{spin}(3)\ , \tag{20}$$

where the twenty-dimensional representation of the $SU^F(4)$ group is chosen. Since the group chain (20) is very similar to the U(6)⊗U(4) group chain (17), one has the same form of the Hamiltonian as in Eq. (18) (of course, with different Casimir operators) and gets the identical formulas for energy levels both in the U(6)×U(4) and U(6)⊗U(20) schemes. The structures of the latter is, however, more rich with more states in the low-energy region. In addition, predictions for the single-particle transfer strength differ in two symmetry limits, the U(6)⊗U(20) scheme being more successful in the Au isotopes.[34]

The wave functions for the U(6)⊗U(20) limit have been obtained by a direct diagonalization of the U(6)⊗U(20) Hamiltonian (18) in the IBFM code ODDA.[35] In the U(6)⊗U(20) limit, we have an ambiguity in four phases Ψ_1, Ψ_2, Ψ_3, and Ψ_4 (for the definition see the Appendix). We have tried to determine the proper phases from microscopic relations. The coefficients $\Gamma_{j_1j_2}$, which appear in the explicitly rewritten Hamiltonian with the terms

$$\Gamma_{j_1j_2}(s^\dagger\tilde{d}+d^\dagger s)^{(2)}\cdot(a^\dagger_{j_1}\tilde{a}_{j_2})^{(2)}\ , \tag{21}$$

are expressed in the microscopic approach as[17,18]

$$\Gamma_{j_1j_2}=\Gamma_0(u_{j_1}u_{j_2}-v_{j_1}v_{j_2})\langle j_1\|Y^{(2)}\|j_2\rangle\ . \tag{22}$$

We cannot, however, fulfill the relations (22) with the Au occupancies from Table III completely for any combination of phases Ψ_1, Ψ_2, Ψ_3, and Ψ_4. In the case $\Psi_1,\Psi_2,\Psi_3,\Psi_4=(+1,-1,+1,+1)$ the signs of the coefficients $\Gamma_{5/25/2}$ and $\Gamma_{5/27/2}=-\Gamma_{7/25/2}$ are opposite to what is suggested from Eq. (22). In the case $\Psi_1,\Psi_2,\Psi_3,\Psi_4=(+1,+1,-1,-1)$ the signs of $\Gamma_{5/25/2}$ and $\Gamma_{3/27/2}=\Gamma_{7/23/2}$ disagree with (22). For the other combinations, the situation is even worse and the microscopic relations are not fulfilled for more Γ's. This fact, together with those required in the U(6)⊗U(20) limit and not obtained from the BCS calculations close values of quasiparticle energies, suggests that to microscopically justify the U(6)⊗U(20) symmetry in the Au region is not an easy task.

D. Odd-proton nuclei—perturbed U(6)⊗U(4) symmetry

The $s_{1/2}$ level, which is not considered in the U(6)⊗U(4) symmetry limit, is certainly important in the low part of spectra of the odd Ir and Au isotopes. The U(6)⊗U(20) symmetry includes the $s_{1/2}$ level, but it overestimates the contribution of the $d_{5/2}$ and $g_{7/2}$ levels. An intermediate approach is, therefore, suggested in which the $d_{3/2}$ and $s_{1/2}$ levels are considered. Cizewski *et al.*[10,34] proposed a method in which the starting point is still the U(6)⊗U(4) Hamiltonian (18) to which a perturbation H_C including the $s_{1/2}$ level is added. The form of the H_C is

$$H_C=\varepsilon_{1/2}n_{1/2}-2\sqrt{5}C(d^\dagger\tilde{d})^{(1)}\cdot(a^\dagger_{1/2}\tilde{a}_{1/2})^{(1)}+\Gamma_{1/23/2}(s^\dagger\tilde{d}+d^\dagger s)^{(2)}\cdot(a^\dagger_{1/2}\tilde{a}_{3/2}-a^\dagger_{3/2}\tilde{a}_{1/2})^{(2)}$$
$$+(\Gamma_{3/23/2}+A/2)(s^\dagger\tilde{d}+d^\dagger s)^{(2)}\cdot(a^\dagger_{3/2}\tilde{a}_{3/2})^{(2)}\ . \tag{23}$$

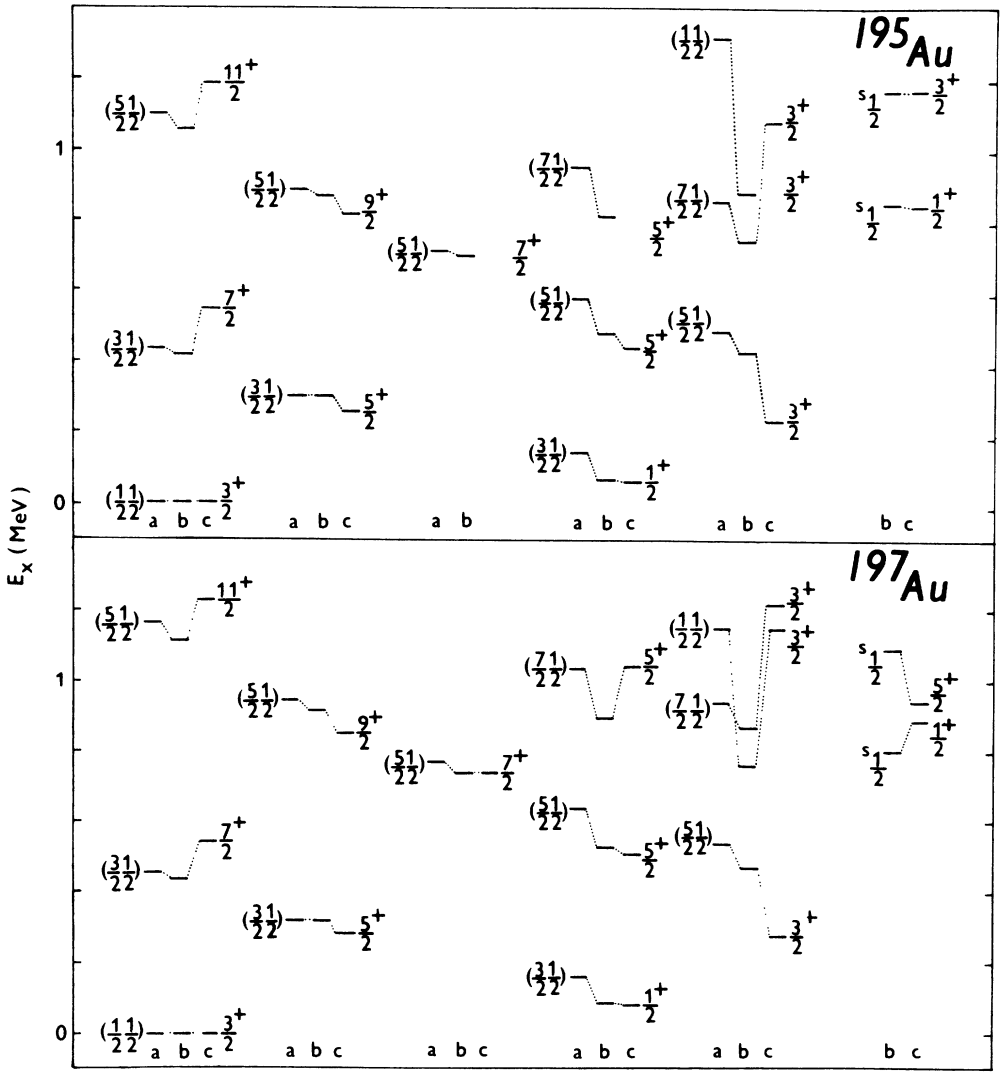

FIG. 3. Energy levels for ^{195}Au and ^{197}Au as predicted by (a) the U(6)⊗U(4) symmetry limit, (b) the perturbed U(6)⊗U(4) scheme, and (c) experimentally observed. Spin is given on the right of level groups, whereas on the left the spin(5) quantum numbers (τ_1,τ_2) are shown. The levels displayed have the spin(6) quantum numbers $\langle\sigma_1,\sigma_2,\sigma_3\rangle=\langle 13/2,1/2,1/2\rangle$ and $\langle 11/2,1/2,1/2\rangle$ for ^{195}Au and ^{197}Au, respectively, with the exception of the $J^\pi(\tau_1,\tau_2)=3/2^+(1/2,1/2)$ level at $E_x\approx 1$ MeV which has $\langle\sigma_1,\sigma_2,\sigma_3\rangle=\langle 11/2,1/2,-1/2\rangle$ and $\langle 9/2,1/2,-1/2\rangle$ for ^{195}Au and ^{197}Au, respectively. The levels marked by $s_{1/2}$ are based mainly on the $s_{1/2}$ level in the perturbed U(6)⊗U(4) scheme and are not present in the U(6)⊗U(4) limit.

TABLE IV. Parameters (in MeV) of calculations in the perturbed U(6)⊗U(4) scheme.

	A	B	C	$\varepsilon_{1/2}-\varepsilon_{3/2}$	$\Gamma_{3/23/2}$	$\Gamma_{1/23/2}$
^{195}Ir	0.184	0.258	0.019	0.70	−0.040	−0.035
^{195}Au	0.329	0.244	0.019	0.50	−0.112	0.058
^{197}Au	0.329	0.269	0.020	0.50	−0.112	0.058

The factor $A/2$ in Eq. (23) subtracts the corresponding part from the U(6)⊗U(4) Hamiltonian (18) so that the notation in Eq. (23) is in agreement with Eq. (21). (The phase convention $\Psi=+1$ discussed in Sec. IV B is adopted.)

Calculations in the perturbed U(6)⊗U(4) scheme for the Ir isotopes were performed in Ref. 10, from where we take the parameters for ^{195}Ir. Similar calculations for the Au isotopes have been, however, less successful.[34] We have, therefore, found new sets of parameters for ^{195}Au and ^{197}Au. The parameters of the calculations in the perturbed U(6)⊗U(4) scheme are shown in Table IV.

Experimental spectra of ^{195}Au and ^{197}Au are compared with the calculations in the U(6)⊗U(4) limit and in the perturbed U(6)⊗U(4) method in Fig. 3. New levels, based mainly on the $s_{1/2}$ state, appear in the perturbed scheme. Otherwise, the level structure in the perturbed method is not changed very much from that of the U(6)⊗U(4) limit. We keep the labeling by the U(6)⊗U(4) quantum numbers also for the levels with a prevailing $d_{3/2}$ component in the perturbed calculations.

Energy levels in the perturbed scheme are invariant under the phases of the parameters $\Gamma_{3/23/2}$ and $\Gamma_{1/23/2}$. In Table IV, the parameter $\Gamma_{3/23/2}$ is negative in agreement with the discussion in Sec. IV B. According to the microscopic relation (22), the parameter $\Gamma_{1/23/2}$ changes the sign when going from the Ir to Au nuclei, being positive for the latter. The ratio of $\Gamma_{1/23/2}$(Ir)/$\Gamma_{1/23/2}$(Au) deduced from Eq. (22) (keeping the same Γ_0) is −0.59 which has to be compared with the value −0.60 from Table IV. The relative values of the parameters $\Gamma_{3/23/2}$ and $\Gamma_{1/23/2}$ agree also with the microscopic estimate reasonably.

V. RESULTS AND DISCUSSION

We have calculated the ft values for beta decay in the $A=195$ and 197 systems. The decays of ^{195}Ir→^{195}Pt, ^{195}Hg→^{195}Au, and ^{197}Hg→^{197}Au are of the first kind with the same even-even core in parent and daughter nuclei [the transition operator (10)]. The decays of ^{195}Au→^{195}Pt and ^{197}Pt→^{197}Au are of the second kind with the change of the proton and neutron boson numbers of the even-even core [the transition operator (11)]. The results are shown and compared with experimental data[36] in Tables V–IX.

The calculations using the perturbed U(6)⊗U(4) approach are the most successful in reproducing experimental results. There are some discrepancies but most of the transitions are explained well in these calculations. With the exception of the transitions from the Hg nuclei to the lowest states in the Au nuclei, the U(6)⊗U(20) results should be preferred in comparison with the U(6)⊗U(4) ones.

The transitions to the $3/2_2^+$ states of odd-proton Au nuclei (Tables VII–IX) are strongly suppressed within the single j-shell U(6)⊗U(4) limit. The transitions to the $1/2_2^+$, $3/2_3^+$, and $3/2_4^+$ states in the ^{195}Hg→^{195}Au decay (Table VII) cannot be explained in this limit at all. The situation is improved considerably when additional shells are included, both in the U(6)⊗U(20) limit and in the perturbed U(6)⊗U(4) scheme. The admixture of the $s_{1/2}$ level in the $3/2_2^+$ state decreases the calculated ft value and brings it to a fair agreement with experiment in the ^{195}Hg→^{195}Au decay. For the transitions to the ^{197}Au($3/2_2^+$) state, the calculated ft values are, however, still greater than the experimental ones. The squared

TABLE V. Experimental and calculated logft values for the ^{195}Ir → ^{195}Pt decay. Results using the U(6)⊗U(4) symmetry limit and the perturbed U(6)⊗U(4) scheme for the ^{195}Ir $3/2^+$ ground state with the U(6)⊗U(4) quantum numbers $\langle\sigma_1,\sigma_2,\sigma_3\rangle(\tau_1,\tau_2)=\langle 13/2,1/2,1/2,\rangle(1/2,1/2)$ are compared. The U(6)⊗U(12) quantum numbers $\langle\sigma_1,\sigma_2\rangle(\tau_1,\tau_2)-L$ for states in ^{195}Pt are also shown. E_x is the experimental excitation energy.

J_f	E_x (keV)	$\langle\sigma_1\sigma_2\rangle(\tau_1\tau_2)-L$	expt.	logft U(6)⊗U(4)	logft U(6)⊗U(4)
$1/2_1^-$	0	⟨70⟩(00)−0	7.0	7.54	7.38
$3/2_1^-$	99	⟨61⟩(10)−2	6.6	7.02	6.74
$5/2_1^-$	130	⟨61⟩(10)−2	6.2	7.35	6.89
$3/2_2^-$	199	⟨61⟩(11)−1		7.26	7.56
$3/2_3^-$	211	⟨70⟩(10)−2	7.2	7.18	6.77
$1/2_2^-$	222	⟨61⟩(11)−1		9.89	8.00
$5/2_2^-$	239	⟨70⟩(10)−2		6.60	6.31

TABLE VI. Experimental and calculated logft values for the ^{195}Au→^{195}Pt decay. Results using the U(6)⊗U(4) symmetry limit, the U(6)⊗U(20) symmetry limit, and the perturbed U(6)⊗U(4) scheme for the ^{195}Au $3/2^+$ ground state are compared. For the ^{195}Au ground state, the spin(5) quantum numbers are $(\tau_1,\tau_2)=(1/2,1/2)$, and the spin(6) quantum numbers are $\langle\sigma_1,\sigma_2,\sigma_3\rangle=\langle 13/2,1/2,1/2\rangle$ and $\langle 15/2,1/2,1/2\rangle$ in the U(6)⊗U(4) and the U(6)⊗U(20) limits, respectively. The U(6)⊗U(12) quantum numbers $\langle\sigma_1,\sigma_2\rangle(\tau_1,\tau_2)-L$ for the states in ^{195}Pt are also shown. E_x is experimental excitation energy.

				logft		
J_f	E_x (keV)	$\langle\sigma_1\sigma_2\rangle(\tau_1\tau_2)-L$	expt.	U(6)⊗U(4)	U(6)⊗U(20)	Perturbed U(6)⊗U(4)
$1/2_1^-$	0	$\langle 70\rangle(00)-0$	8.1	8.30	8.30	8.22
$3/2_1^-$	99	$\langle 61\rangle(10)-2$	6.54	6.56	6.54	6.45
$5/2_1^-$	130	$\langle 61\rangle(10)-2$	6.36	6.06	6.06	6.00
$3/2_2^-$	199	$\langle 61\rangle(11)-1$	8.32	7.18	7.49	7.31
$3/2_3^-$	211	$\langle 70\rangle(10)-2$	7.46	7.37	7.39	7.16

TABLE VII. Experimental and calculated logft values for the ^{195}Hg→^{195}Au decay. Results using the U(6)⊗U(4) symmetry limit, the U(6)⊗U(20) symmetry limit, and the perturbed U(6)⊗U(4) scheme for states in ^{195}Au, and the U(6)⊗U(12) symmetry with the SO(6) subgroup and the U(5) subgroup for the ^{195}Hg $1/2^-$ ground state are compared. The ^{195}Hg ground state belongs to the $\{n_1n_2\}=\{00\}$ irrep of the U^{BF}(5) subgroup or to the $\langle\sigma_1\sigma_2\rangle=\langle 70\rangle$ irrep of the SO^{BF}(6) subgroup, the SO^{BF}(5) and SO^{BF}(3) numbers being $(\tau_1\tau_2)-L=(00)-0$ in both limits. The states $1/2_2^+$ and $3/2_4^+$ of ^{195}Au are based mainly on the $s_{1/2}$ level; in the U(6)⊗U(20) limit, they have the spin(6) numbers $\langle\sigma_1,\sigma_2,\sigma_3\rangle=\langle 13/2,3/2,1/2\rangle$. The other ^{195}Au states have the spin(6) numbers $\langle 13/2,1/2,1/2\rangle$ and $\langle 15/2,1/2,1/2\rangle$ for the U(6)⊗U(4) and U(6)⊗U(20) limits, respectively. The spin(5) numbers (τ_1,τ_2) are also shown. E_x is the experimental excitation energy.

				logft					
				Hg-SO^{BF}(6)			Hg-U^{BF}(5)		
J_f	E_x (keV)	$(\tau_1\tau_2)$	expt.	U(6)⊗U(4)	U(6)⊗U(20)	Perturbed U(6)⊗U(4)	U(6)⊗U(4)	U(6)⊗U(20)	Perturbed U(6)⊗U(4)
$3/2_1^+$	0	(1/2 1/2)	7.3	7.22	8.48	7.41	8.24	8.60	8.61
$1/2_1^+$	62	(3/2 1/2)	6.4	6.06	6.52	6.42	6.62	6.74	6.84
$3/2_2^+$	242	(5/2 1/2)	7.9	10.41	7.91	7.82	∞	8.29	8.68
$1/2_2^+$	841	(3/2 1/2)	6.6		7.12	6.49		7.71	7.19
$3/2_3^+$	1083	(7/2 1/2)	7.2	∞	7.48	12.27	∞	∞	11.22
$3/2_4^+$	1172	(3/2 3/2)	6.4		7.30	6.80		7.63	7.71

TABLE VIII. Experimental and calculated logft values for the ^{197}Pt→^{197}Au decay. Results using the U(6)⊗U(4) symmetry limit, the U(6)⊗U(20) symmetry limit, and the perturbed U(6)⊗U(4) scheme for states in ^{197}Au are compared. The U(6)⊗U(12) quantum numbers for the ^{197}Pt $1/2^-$ ground state are $\langle\sigma_1\sigma_2\rangle(\tau_1\tau_2)-L=\langle 60\rangle(00)-0$. The spin(6) numbers for the ^{197}Au states are $\langle\sigma_1\sigma_2\sigma_3\rangle=\langle 11/2,1/2,1/2\rangle$ and $\langle 13/2,1/2,1/2\rangle$ for the U(6)⊗U(4) and U(6)⊗U(20) limits, respectively. The spin(5) numbers $(\tau_1\tau_2)$ are also shown. E_x is the experimental excitation energy.

				logft		
J_f	E_x (keV)	$(\tau_1\tau_2)$	expt.	U(6)⊗U(4)	U(6)⊗U(20)	Perturbed U(6)⊗U(4)
$3/2_1^+$	0	(1/2 1/2)	7.3	8.20	7.91	7.94
$1/2_1^+$	77	(3/2 1/2)	6.3	6.69	6.47	6.37
$3/2_2^+$	269	(5/2 1/2)	6.8	11.93	8.33	8.38

TABLE IX. Experimental and calculated logft values for ^{197}Hg→^{197}Au decay. Results using the U(6)⊗U(4) symmetry limit, the U(6)⊗U(20) symmetry limit, and the perturbed U(6)⊗U(4) scheme for states in ^{197}Au, and the U(6)⊗U(12) symmetry with the SO(6) subgroup and the U(5) subgroup for the ^{197}Hg $1/2^-$ ground state are compared. The ^{197}Hg ground state belongs to the $\{n_1 n_2\}=\{00\}$ irrep of the U^{BF}(5) subgroup or to the $\langle\sigma_1\sigma_2\rangle=\langle 60\rangle$ irrep of the SO^{BF}(6) subgroup, the SO^{BF}(5) and SO^{BF}(3) numbers being $(\tau_1\tau_2)-L=(00)-0$ in both limits. The spin(6) numbers for the ^{197}Au states are $\langle\sigma_1\sigma_2\sigma_3\rangle=\langle 11/2,1/2,1/2\rangle$ and $\langle 13/2,1/2,1/2\rangle$ for the U(6)⊗U(4) and U(6)⊗U(20) limits, respectively. The spin(5) numbers $(\tau_1\tau_2)$ are also shown. E_x is the experimental excitation energy.

			logft					
				Hg-SO^{BF}(6)		Hg-U^{BF}(5)		
J_f	E_x (keV)	$(\tau_1\tau_2)$	expt.	U(6)⊗U(4)	U(6)⊗U(20)	Perturbed U(6)⊗U(4)	U(6)⊗U(4)	U(6)⊗U(20)	Perturbed U(6)⊗U(4)
$3/2_1^+$	0	(1/2 1/2)	7.2	7.03	8.75	7.19	7.78	8.78	7.99
$1/2_1^+$	77	(3/2 1/2)	5.71	5.94	6.36	6.28	6.46	6.63	6.72
$3/2_2^+$	269	(5/2 1/2)	6.60	9.05	7.68	7.60	∞	7.83	8.51

overlap of the ^{195}Au$(3/2_2^+)$ wave functions in the U(6)⊗U(4) limit and in the perturbed U(6)⊗U(4) method is 0.89 which shows that the admixture of the $s_{1/2}$ orbit is not large in the perturbed approach. Nevertheless, even this admixture causes an increase in the beta decay transition rate by a factor of about 20.

A huge discrepancy occurs for the transition ^{195}Hg→^{195}Au$(3/2_3^+)$ (Table VII) in the perturbed U(6)⊗U(4) scheme. On the other hand, satisfactory results for this transition are obtained with the U(6)⊗U(20) limit. This suggests that for the $3/2_3^+$ level, the inclusion of further single-particle levels, and particularly of the $d_{5/2}$ level, might be important.

A strong beta transition to the $3/2_4^+$ level at $E=1.172$ MeV is observed in the ^{195}Hg→^{195}Au decay with the experimental log$ft=6.4$. In Ref. 33 this level has been related to the

$$\langle\sigma_1,\sigma_2,\sigma_3\rangle(\tau_1,\tau_2)=\langle 13/2,1/2,-1/2\rangle(1/2,1/2)$$

level of the U(6)⊗U(20) limit, $\langle\sigma_1,\sigma_2,\sigma_3\rangle$ and (τ_1,τ_2) being the spin (6) and spin (5) quantum numbers, respectively. The calculated logft value is then 9.17. A small ft value in this energy region is obtained only for the state

$$\langle\sigma_1,\sigma_2,\sigma_3\rangle(\tau_1,\tau_2)=\langle\tfrac{13}{2},\tfrac{3}{2},\tfrac{1}{2}\rangle(\tfrac{3}{2},\tfrac{3}{2})$$

in the U(6)⊗U(20) limit with a large $s_{1/2}$ component or for a state in the perturbed U(6)⊗U(4) scheme based mainly on the $s_{1/2}$ level. We identify, therefore, these states with the experimental 1.172 level.

The results with two different descriptions of the Hg ground state, based on the group chains with either the SO(6) [Eq. (14)] or the U(5) [Eq. (15)] subgroups, are compared in Tables VII and IX. The SO(6) limit is apparently preferable to the U(5) limit. For the latter, the resulting ft values are too large. This is understandable as in the description of odd-proton Au nuclei the SO(6) symmetry of the even-even core is assumed which implies small overlaps between the Au and the Hg [U(5)] wave functions. We note that from the IBFM point of view the wave functions of the even-even core should be the same in odd-proton and odd-neutron nuclei. The U(5) limit for the Hg nuclei might give more satisfactory results for beta decay rates in combination with the Au wave functions based also on the U(5) limit.[26] Then however, the results for the Pt↔Au transitions would deteriorate.

The ft values for the transitions in the ^{195}Au→^{195}Pt decay (Table VI) are well reproduced with the exception of the transition to the $3/2_2^-$ state. The transitions with the experimentally known ft value in the ^{195}Ir→^{195}Pt decay (Table V) are calculated also satisfactorily. Difficulties seem to appear in the ^{195}Ir→^{195}Pt decay for

TABLE X. Experimental and calculated logft values for transitions to two lowest states. The U(6)⊗U(4) symmetry limit is used for odd-proton nuclei. Results for different combinations of the U(6)⊗U(12) phase ϕ and the U(6)⊗U(4) phase Ψ are compared.

			logft			
	J_f	expt.	$\phi=-1$ $\Psi=+1$	$\phi=+1$ $\Psi=+1$	$\phi=-1$ $\Psi=-1$	$\phi=+1$ $\Psi=-1$
^{195}Ir→^{195}Pt	$1/2_1^-$	7.0	7.54	9.06	7.34	8.35
	$3/2_1^-$	6.6	7.02	6.79	6.16	6.02
^{195}Au→^{195}Pt	$1/2_1^-$	8.1	8.30	7.52	9.34	7.80
	$3/2_1^-$	6.54	6.56	7.15	7.40	9.36
^{195}Hg→^{195}Au	$3/2_1^+$	7.3	7.22	9.91	7.00	8.09
	$1/2_1^+$	6.4	6.06	6.59	5.55	7.18
^{197}Pt→^{197}Au	$3/2_1^+$	7.3	8.20	7.34	10.74	7.49
	$1/2_1^+$	6.3	6.69	5.94	6.29	6.19
^{197}Hg→^{197}Au	$3/2_1^+$	7.2	7.03	8.86	7.00	8.16
	$1/2_1^+$	5.71	5.94	6.74	5.57	7.45

the transitions to the $3/2_2^-$, $1/2_2^-$, and $5/2_2^-$ states which are not experimentally observed and for which the ft values are presumably large. Theory predicts that these transitions, and especially the transition to the $5/2_2^-$ final state, are rather strong. A large sensitivity to details of nuclear wave functions can be again traced in calculations of beta decay rates. For example, the squared overlap of the ^{195}Ir (g.s.) wave functions in the U(6)⊗U(4) symmetry and the perturbed U(6)⊗U(4) scheme is 0.96. The calculated ft values in two approaches differ for the transitions to the ^{195}Pt($5/2_1^-$) and ^{195}Pt($1/2_2^-$) states by factors of 2.9 and 78, respectively.

The ft values for the transitions to two lowest states calculated with the U(6)⊗U(4) wave functions are collected in Table X. The results for various combinations of the U(6)⊗U(12) phase ϕ and the U(6)⊗U(4) phase Ψ are compared. We remind that energy levels are invariant and electromagnetic transition probabilities do not change much under these phases. The microscopically suggested combination $(\phi,\Psi)=(-1,+1)$ is preferred from comparison with experiment.

In the case of the U(6)⊗U(20) wave functions, two microscopically most favorable combinations of phases $(\Psi_1,\Psi_2,\Psi_3,\Psi_4)=(+1,-1,+1,+1)$ and $(+1,+1,-1,-1)$ give close results, the former combination being used in Tables VI–IX. The calculated ft values for the other combination of phases are less successful in reproducing experiment than those shown in the tables.

The ft values for the transitions to two lowest states calculated with the perturbed U(6)⊗U(4) method are displayed in Table XI. The values in column A of Table XI repeat only those of Tables V–IX. They are obtained with the parameters of the perturbed method as given by microscopic considerations and shown in Table IV. The results in column B are from the calculations in which the sign of the parameter $\Gamma_{1/2\,3/2}$ is taken opposite to that of Table IV. Such a sign change implies a change of the relative sign of the $s_{1/2}$ and $d_{3/2}$ components in the wave functions. This leaves the calculated energies invariant. The calculated ft values in columns A and B of Table IV differ with a preference for the microscopically indicated parameters.

In column C of Table XI, the ft values are shown as obtained when only the direct term ($\sim a^\dagger\tilde{a}$) is considered in the IBFM beta transition operators (10) and (11) [the nuclear wave functions are the same as in column A]. The differences between columns A and C are considerable in most cases. The results in column A reproduce experimental data undoubtedly better than those in column C. Exchange terms in the transition operators are therefore quite important for beta decay calculations. Inclusion of them brings the calculated ft values to a better agreement with experiment.

VI. CONCLUSIONS

The ft values have been calculated for a relatively large sample of 24 first nonunique forbidden transitions in the $A=195$ and 197 nuclei within the framework of the IBFM. Experimental data for most transitions have been reproduced rather well. Nevertheless, discrepancies remain for some transitions. On the whole, however, the agreement between theory and experiment in the present study seems to be better than that obtained usually in previous beta decay studies in regions of collective nuclei.

The calculated beta decay rates are very sensitive to details of nuclear wave functions. Even small admixtures in the wave functions can change the resulting ft values considerably. This makes beta decay a powerful tool for testing nuclear structure. In the present study, the best results have been obtained when the perturbed U(6)⊗U(4) scheme has been applied to odd-proton nuclei pointing out the importance of the proton $s_{1/2}$ shell in the region studied. We have also been able to discriminate between different phases of nuclear wave functions under which energy levels are invariant and which cannot be easily disentangled from electromagnetic transition probabilities. It is pleasing that the microscopically deduced phases provide the best explanation of experiment.

It is likely that our knowledge of nuclear states is still incomplete for the transitions which have not been reproduced well. Especially, the influence of the proton $d_{5/2}$ shell might be important. In any case, dependence of calculated beta decay rates on nuclear wave functions

TABLE XI. Experimental and calculated logft values for transitions to two lowest states. The perturbed U(6)⊗U(4) scheme is used for odd-proton nuclei. The results in column A are with parameters as given in Table IV. The results in column B are with the sign of the parameter $\Gamma_{1/2\,3/2}$ opposite to that of Table IV. The results in column C are obtained with the same wave functions as in column A when only the direct term is considered in the IBFM beta transition operator.

			logft		
	J_f	expt.	A	B	C
^{195}Ir→^{195}Pt	$1/2_1^-$	7.0	7.38	7.51	8.30
	$3/2_1^-$	6.6	6.74	6.82	6.32
^{195}Au→^{195}Pt	$1/2_1^-$	8.1	8.22	8.57	8.21
	$3/2_1^-$	6.54	6.45	6.73	7.09
^{195}Hg→^{195}Au	$3/2_1^+$	7.3	7.41	7.00	8.70
	$1/2_1^+$	6.4	6.42	5.68	6.80
^{197}Pt→^{197}Au	$3/2_1^+$	7.3	7.94	8.70	7.90
	$1/2_1^+$	6.3	6.37	6.97	7.14
^{197}Hg→^{197}Au	$3/2_1^+$	7.2	7.19	6.86	8.19
	$1/2_1^+$	5.71	6.28	5.60	6.78

should be carefully investigated before the higher order effects in beta decay theory are called for an explanation of some transitions.

The exchange terms in the IBFM beta transition operators proved to be quite important. They take into account the Pauli principle between the odd nucleon and nucleons which form the even-even collective core. The state of the core is changed by the action of the exchange terms. Such terms have not been usually considered in other collective model approaches. The microscopic interpretation of the IBFM enables us to evaluate the exchange terms explicitly so that we have no free parameter in the IBFM transition operator. The calculated ft values reproduce experiment satisfactorily only when the contribution of the exchange terms is included. This fact strengthens the usefulness of beta decay in testing nuclear structure as both single-particle and collective degrees of freedom are involved in beta decay processes.

The role of the exchange terms in beta decay suggests that such terms might be important also in single-nucleon transfer. Analyses of single-nucleon structure in which only the direct terms of the transition operator (9) are taken into account should be, therefore, regarded with caution.

On the other hand, importance of the exchange terms leaves an unanswered question about an effect of higher order terms neglected in the single-nucleon transfer and beta transition operators (9)–(11). A full and consistent evaluation of these effects represents a rather difficult problem and has not been done till now.

ACKNOWLEDGMENT

We would like to thank M. Ryšavý, O. Scholten, and E. Truhlík for useful discussions.

APPENDIX

The Casimir operators in Eq. (18) are written in terms of the group generators $G^{(1)}$, $G^{(2)}$, and $G^{(3)}$ as

$$C_3 = 10G^{(1)}\cdot G^{(1)} ,$$

$$C_5 = \tfrac{1}{3}(G^{(1)}\cdot G^{(1)} + G^{(3)}\cdot G^{(3)}) ,$$

$$C_6 = \tfrac{1}{2}(\tfrac{1}{2}G^{(2)}\cdot G^{(2)} + G^{(1)}\cdot G^{(1)} + G^{(3)}\cdot G^{(3)}) .$$

For the U(6)⊗U(20) limit, the generators are given as

$$G^{(1)} = (d^\dagger \tilde{d})^{(1)} - \sqrt{1/20}(a^\dagger_{1/2}\tilde{a}_{1/2})^{(1)} - \sqrt{1/2}(a^\dagger_{3/2}\tilde{a}_{3/2})^{(1)} - \sqrt{7/2}(a^\dagger_{5/2}\tilde{a}_{5/2})^{(1)} - \sqrt{21/5}(a^\dagger_{7/2}\tilde{a}_{7/2})^{(1)} ,$$

$$\begin{aligned} G^{(2)} = {} & (d^\dagger s + s^\dagger \tilde{d})^{(2)} + \sqrt{6/7}\Psi_1(a^\dagger_{7/2}\tilde{a}_{7/2})^{(2)} - \tfrac{1}{5}\sqrt{3/7}\Psi_1(a^\dagger_{5/2}\tilde{a}_{5/2})^{(2)} + \tfrac{7}{5}\Psi_1(a^\dagger_{3/2}\tilde{a}_{3/2})^{(2)} \\ & - \tfrac{1}{5}\sqrt{21/2}\Psi_1\Psi_3\Psi_4(a^\dagger_{1/2}\tilde{a}_{5/2} + a^\dagger_{5/2}\tilde{a}_{1/2})^{(2)} + (12/5\sqrt{7})\Psi_1\Psi_4(a^\dagger_{5/2}\tilde{a}_{7/2} - a^\dagger_{7/2}\tilde{a}_{5/2})^{(2)} \\ & + (2\sqrt{3}/5)\Psi_2\Psi_3(a^\dagger_{1/2}\tilde{a}_{3/2} - a^\dagger_{3/2}\tilde{a}_{1/2})^{(2)} + \tfrac{6}{5}\Psi_2\Psi_4(a^\dagger_{3/2}\tilde{a}_{5/2} - a^\dagger_{5/2}\tilde{a}_{3/2})^{(2)} \\ & + (4\sqrt{3}/5)\Psi_2(a^\dagger_{3/2}\tilde{a}_{7/2} + a^\dagger_{7/2}\tilde{a}_{3/2})^{(2)} , \end{aligned}$$

$$\begin{aligned} G^{(3)} = {} & (d^\dagger \tilde{d})^{(3)} + \frac{1}{\sqrt{2}}(a^\dagger_{3/2}\tilde{a}_{3/2})^{(3)} - (3/7\sqrt{2})(a^\dagger_{5/2}\tilde{a}_{5/2})^{(3)} - \tfrac{1}{7}\sqrt{33/5}(a^\dagger_{7/2}\tilde{a}_{7/2})^{(3)} \\ & + \tfrac{1}{2}\sqrt{15/7}\Psi_3\Psi_4(a^\dagger_{1/2}\tilde{a}_{5/2} + a^\dagger_{5/2}\tilde{a}_{1/2})^{(3)} + \tfrac{6}{7}\sqrt{5/2}\Psi_4(a^\dagger_{5/2}\tilde{a}_{7/2} - a^\dagger_{7/2}\tilde{a}_{5/2})^{(3)} \\ & - (6/\sqrt{70})\Psi_3(a^\dagger_{1/2}\tilde{a}_{7/2} - a^\dagger_{7/2}\tilde{a}_{1/2})^{(3)} \end{aligned}$$

with the phases Ψ_1, Ψ_2, Ψ_3, and Ψ_4 equal to ± 1.

[1] A. Arima and F. Iachello, Adv. Nucl. Phys. **13**, 139 (1983).
[2] F. Iachello and O. Scholten, Phys. Rev. Lett. **43**, 679 (1979).
[3] O. Scholten and Z. R. Yu, Phys. Lett. **161B**, 13 (1985).
[4] H. Behrens and W. Bühring, *Electron Radial Wave Functions and Nuclear Beta-decay* (Clarendon, Oxford, 1982).
[5] D. Bogdan, A. Faessler, P. Vertes, and H. Toki, Nucl. Phys. **A321**, 438 (1979).
[6] J. A. Cizewski *et al.*, Nucl. Phys. **A323**, 349 (1979); R. F. Casten and J. A. Cizewski, Phys. Lett. B **185**, 293 (1987).
[7] F. Iachello and S. Kuyucak, Ann. Phys. (N.Y.) **136**, 19 (1981).
[8] A. B. Balantekin, I. Bars, R. Bijker, and F. Iachello, Phys. Rev. C **27**, 1761 (1983).
[9] Y. S. Ling *et al.*, Phys. Lett. **148B**, 13 (1984).
[10] J. A. Cizewski *et al.*, Phys. Rev. C **27**, 1040 (1983).
[11] S. Nozawa, K. Kubodera, and H. Ohtsubo, Nucl. Phys. **A453**, 645 (1986); I. S. Towner, Ann. Rev. Nucl. Part. Sci. **36**, 115 (1986); M. Kirchbach and E. Truhlík, Sov. J. Fiz. Elem. Chastits. At. Yadra **17**, 224 (1986); M. Kirchbach, Nucl. Phys. **A465**, 705 (1987).
[12] J. Damgaard, R. Broglia, and C. Riedel, Nucl. Phys. **A135**, 310 (1969).
[13] I. S. Batkin, I. M. Berman, and I. V. Kopytin, Yad. Fiz. **23**,

564 (1976) [Sov. J. Nucl. Phys. **23**, 296 (1976)].
[14]H. Ejiri and J. I. Fujita, Phys. Rep. **38C**, 85 (1978).
[15]F. Krmpotic, K. Ebert, and W. Wild, Nucl. Phys. **A342**, 497 (1980).
[16]K. Bear and P. E. Hodgson, J. Phys. G **4**, L287 (1978).
[17]O. Scholten, Ph.D. thesis, University of Groningen, 1980.
[18]O. Scholten and A. E. L. Dieperink, in *Interacting Bose-Fermi Systems in Nuclei,* edited by F. Iachello (Plenum, New York, 1981), p. 343.
[19]P. Ring and P. Schuck, *The Nuclar Many-Body Problem* (Springer-Verlag, New York, 1980), Chap. 6.
[20]R. Bijker and O. Scholten, Phys. Rev. C **32**, 591 (1985).
[21]A. Bohr and B. R. Mottelson, *Nuclear Structure* (Benjamin, New York, 1975), Vol. 2, Chap. 5.3.2.
[22]R. Bijker and A. E. L. Dieperink, Nucl. Phys. **A379**, 221 (1982).
[23]P. Van Isacker, A. Frank, and H. Z. Sun, Ann. Phys. (N.Y.) **157**, 183 (1984).
[24]R. Bijker and F. Iachello, Ann. Phys. (N.Y.) **161**, 360 (1985).
[25]A. Mauthofer *et al.*, Phys. Rev. C **24**, 1958 (1986), and unpublished.
[26]P. B. Semmes, A. F. Barfield, B. R. Barrett, and J. L. Wood, Phys. Rev. C **35**, 844 (1987).
[27]M. Vergnes *et al.*, Phys. Rev. C **31**, 2071 (1985).
[28]P. Van Isacker, A. Frank, and J. Dukelsky, Phys. Rev. C **31**, 671 (1985).
[29]O. Scholten, S. Brant, and V. Paar, Phys. Lett. B **171**, 335 (1986).
[30]J. A. Cizewski *et al.*, Phys. Rev. Lett. **58**, 10 (1987).
[31]J. L. Wood, in *Interacting Bose-Fermi Systems in Nuclei,* edited by F. Iachello (Plenum, New York, 1981), p. 381.
[32]J. Vervier, Phys. Lett. **100B**, 383 (1981); J. Vervier *et al.*, *ibid.* **105B**, 343 (1981).
[33]M. Vallieres, in *Interacting Boson-Boson and Boson-Fermion Systems,* edited by O. Scholten (World-Scientific, Singapore, 1984), p. 120.
[34]J. A. Cizewski, in *Interacting Boson-Boson and Boson-Fermion Systems,* edited by O. Scholten (World-Scientific, Singapore, 1984), p. 103.
[35]O. Scholten, Program ODDA, University of Groningen Report KVI-252, 1981.
[36]B. Harmatz, Nucl. Data Sheets **23**, 607 (1978); B. Harmatz, *ibid.* **34**, 101 (1981).